JREE: Vol. 9, No. 3, (Summer 2022) 17-31

Journal of Renewable Energy and Environment

Journal Homepage: www.jree.ir

Materials and Energy Research Center

MERC

Research Article

Modified Concrete for Impeding Chloride Diffusion from Sea Water in the Marine Environment

Davar Rezakhani [a], Abdol Hamid Jafari [a*], Mohammad Ali Hajabassi [b]

[a] *Department of Materials Science and Technology, Shahid Bahonar University,Kerman, Kerman, Iran.*
[b] *Department of Mechanical Engineering, Shahid Bahonar University, Kerman, Kerman, Iran.*

PAPER INFO

Paper history:
Received: 11 July 2021
Revised in revised form: 17 January 2022
Scientific Accepted: 25 September 2021
Published: 11 May 2022

Keywords:
Chloride,
Diffusion,
Graphene Oxide,
Marine Environment,
Ground Granulated Blast Furnace Slag

ABSTRACT

The application of nanomaterials to concrete is an innovative approach to enhance mechanical properties and durability performances. In this work, the addition of a combination of Graphene Oxide Nano-Platelets (GONP) and Ground Granulated Blast Furnace Slag (GGBFS) was studied as admixture in concrete. Tests on mechanical and chloride permeation properties were conducted. The results showed that the mix with 0.05 % GONP and the mix with 30 % GGBFS obtained better mechanical strength than the rest of the mixes. The highest electrical resistivity was achieved for the 90-day cured sample with 50 % GGBFS in CONP-free concrete and the 0.01 % GONP in GGBFS-free concrete, which was found to be the most effective in increasing concrete resistance to chloride permeation. The mix with 0.1 w % GONP and 50 w % GGBFS exhibited considerable performance even with other mechanical and durability performances. The addition of 0.1 % graphene oxide and 50 % granular slag increased the compressive strength of the concrete sample by 19.9 % during 28 days and 17.6 % during 90 days compared to the conventional concrete sample. Concrete with a combination of 0.1 % graphene oxide and 50 % granular slag experienced an increase in flexural strength by 15 % during 28 days and 13.6 % during 90 days. A significant reduction in electrical conductivity from 4012C to 1200C was observed for 90-day cured samples containing 0.1 wt % GO and 50 wt % GGBFS compared to the conventional sample. Response Surface Method (RSM) applied to the test data presented an optimized concrete mix containing 0.08 w % GONP and 50 w % GGBFS, the outcome of which was in close agreement with the experimental results.

https://doi.org/10.30501/jree.2022.293613.1227

1. INTRODUCTION

Concrete remains the most widely used industrial material and new-found modifiers help improve its durability, mechanical properties, and specifically corrosion resistance [1, 2]. An important issue about marine structures is chloride permeation causing rapid rebar corrosion and interference in protection systems including cathodic protection so much so that it has been reported to be the main problem in concrete structures worldwide [3-8]. Even inland, temperature, and humidity fluctuations causing cyclic expansion-contraction and hydration-dehydration could cause the initiation and propagation of cracks in concrete, instigating rebar corrosion and concrete spalling with the subsequent loss of load-bearing capacity. In a chloride-containing environment, its permeation from solution-filled pores, chlorine contaminated cement, or diffusion along paths in the matrix of the concrete may exacerbate the rate of deterioration manifold. Total amount of chloride in concrete consists of bound and free chlorides and the latter is responsible for breaking the passive layer on the bars [9, 10]. In effect, the level of chloride bound to concrete could directly affect corrosion as these immobile ions diminish the overall diffusion rate and accumulation of Cl^- at the rebar-concrete interface [11, 12]. The rate of chlorine ion permeation depends on the materials used and the production parameters such as water-to-cement ratio, additives, and degree of hydration [13].

The application of nanomaterials to concrete is an innovative approach to enhancing its mechanical and durability properties. Nanomaterials in concrete have many advantages including the enhancement of mechanical strength and filling of the voids at a nano level. Concrete has pores on both nano (10^{-9} m) and micro (10^{-6} m) scales. Compaction of concrete reduces the amount of porosity. However, small cavities remain in the concrete composite. The strength of concrete depends on the formation of calcium hydrate silicate products (C-S-H), and the products are pore-dependent at nano and micro levels. Filling of these pores with inert or reactive materials can increase the strength and durability properties, reduce crack formation, and so on. Upon applying pozzolanic materials to concrete, it can only fill small cavities. Therefore, nanometer pores can be filled using these nanomaterials [14, 15]. Nanoparticles react with calcium

*Corresponding Author's Email: jafham2020@gmail.com (A.H. Jafari)
URL: https://www.jree.ir/article_149660.html

Please cite this article as: Rezakhani, D., Jafari, A.H. and Hajabassi, M.A., "Modified concrete for impeding chloride diffusion from sea water in the marine environment", ***Journal of Renewable Energy and Environment (JREE)***, Vol. 9, No. 3, (2022), 17-31. (https://doi.org/10.30501/jree.2022.293613.1227).

hydroxide ($Ca(OH)_2$) and CSH gels in the pores. This measure creates a denser structure and fills pores on the cement [15]. Many researchers have studied the mechanical and durability properties of concrete with nano admixtures and as usual, it exhibits better results than conventional cement composites [16, 17]. A large number of researchers have demonstrated the incorporation of nanomaterials. In recent years, carbon nanomaterials such as Carbon Nanotubes (CNTs), Carbon Nanofibers (CNFs), and Graphene Oxide (GO) have attracted the attention of many concrete researchers due to their unique mechanical, thermal, chemical, and electrical properties [18-20]. However, the application of materials such as carbon nanotube is difficult due to their poor dispersibility. GO sheets with oxygenated functions are more accessible to cement particles, thus allowing nano sheets to act as cores for cement phases and increase the reaction of cement with water [21]. Graphene oxide nano plates have been studied because of their hydrophobic effect at low concentrations [22-26]. Graphene oxide contains functional oxygen groups in its layered structure that increase the inter-planar space causing easier thinning out in aqueous environments. It has been reported that admixing of GO nano plates to cement expedites its hydration process and increases the total hydration products [26]. This has been attributed to its high surface energy that facilitates the absorption of hydration products that acts as nucleation sites for hydration reaction [25]. Yang et al. reported that with the addition of 0.1 wt % GO, cement hydration increased by 10.4 % on Day 28 [27]. Graphene oxide nano particle effect on cement hydration could change the intra-structural porosity with a subsequent increase in cement strength and toughness. Wang et al. maintained that the microstructure of the GO-reinforced cement matrix had a massive crystal structure covering, implying that leaching of Calcium Hydroxide (CH) during the hydration stages was enhanced on Day 28 (curing age) [28]. Addition of GO to cement-based composites has an adverse effect on performance due to its large area that tends to absorb more water molecules for wetting and its large high-capacity lateral size due to the clustering of GO nanoplates [29, 30]. Regardless of the disadvantages mentioned above, combining a small amount of GO at about 1 % by weight of cement improves the compressive strength by 63 % [31]. Lu et al. confirmed that the addition of only 0.05 wt % nano-sized graphene oxide caused 10.4 % and 12.6 % improvements in compressive and flexural strengths after 28 days. Other researchers claimed the improvement rates of 78.6 %, 60.7 %, and 38.9 % in tensile, flexural, and compressive strengths, respectively, by 0.03 % GO addition [32, 33]. Gang Xu et al. reported a 29 % increase in the compressive strength of cement pastes after 28-day curing by admixing 0.02 wt % GO [26]. Hue peng et al. pointed to a 21.86 % increase in flexural strength and overall toughness by admixing 0.03 wt % GO with the cement [25]. The addition of 0.05 % GO was reported to enhance the compressive strength by 15-33 % and flexural strength by 41-58 % [17, 34]. Shang et al. stated that the compressive strength with the inclusion of 0.04 % GO to the cement paste was enhanced by 15.1 % compared to the plain cement paste [35]. The compressive and tensile strengths increased by over 40 % with the inclusion of 0.03 % GO by weight of cement to OPC (Ordinary Portland Cement) paste on Day 28 at the curing age [36]. In the research done by Lee et al., cementitious composites replaced with conventional cement additives, such as Fly Ash (FA), Silica Fume (SF), Nano-Silica (NS), and Ground Granulated Blast-furnace Slag (GGBS) and graphene oxide were studied for comparison. The cementitious composites replaced with GO had compressive strength of 10.6–41.5 % higher than that of the plain mixture and also, higher than that obtained with other cement additives. In this study, the pore structure analysis revealed that the majority of pores had micro pores with diameters not exceeding 2.5 nm which improved their strength [37]. Kudžma et al. studied the effect of graphene oxide with low oxygen content on Portland cement based composites. In this study, the amounts of GO investigated were 0.02 %, 0.04 %, and 0.06 % by weight of cement, while for mortars, an extra composition with 0.1 % was also prepared. According to the results, the fluidity of cement paste and mortar increased and the hydration process was slightly retarded with the addition of GO. However, improvements in compressive and flexural strength were established in the mortars containing GO. The maximum effects (~ 22 % and ~ 6 %, respectively) were obtained with the addition of 0.06 % GO [38].

Hassani et al. used a dose of 0.1 to 2 % GO and observed that high bond strength was created due to the nuclearization of C-S-H by GO shells. As demonstrated by the results, there was an increase in the amount of C-S-H gel which helps reduce the permeability of concrete and increase the durability of concrete structures [39]. Gong et al. studied the effect of GO admixture on cement paste with an optimal dose of GO 0.03 % by weight of cement and found that due to the reduction of the cavity structure, the mechanical strength increased by more than 40 % compared to the conventional matrix [36]. They observed changes in efficiency, heat of hydration, and cavity structures. Analysis of pore structure indicated that the total porosity and capillary pores were reduced by 13.5 % and 27.7 % and gel pores increased. According to the results of this study, more C-S-H products are produced, leading to a reduction in capillary pores and an increase in gel pores. Wang et al. used 0.02, 0.04, 0.06 and 0.08 % Graphene oxides. At 0.08 % dosage, the flexural strength and compressive strength were at maximum, i.e., increased by 27 % and 16.4 %, respectively. They observed that at low amounts of graphene oxide, hydration products bound to each other and remained in specific locations, and when the dose increased, the hydration product would tend to form clusters such as structure to prevent the propagation of small cracks [40]. Kai Guo et al. investigated the impact of GO on chloride penetration resistance of concrete and demonstrated that the addition of 0.06 wt % GO nano plates was enough to achieve the highest chloride penetration resistance [23]. Therefore, previous studies have shown that the chances of improving the mechanical properties, permeability, and durability of cement when using graphene oxide are higher. The required dose of GO is lower than other nanomaterials to obtain the same effect [41, 42].

Other nano-sized additives such as Ground Granulated Blast furnace Slag-GGBFS are mainly used to reduce free chloride by binding it to concrete [43-48]. GGBFS is a by-product of iron production in the blast furnaces where slag is water or steam quenched and ground to a fine mesh powder [49]. Researchers report the beneficial effect of GGBFS on compressive strength while adversely affecting the hydration rate, thus prolonging the time to attain maximum mechanical strength [50-52]. Chen et al. reported the effect of around 45 wt % GGBFS on reducing the chloride penetration [53]. Samad et al. found that GGBS concrete gained much more strength than the Portland cement concrete until 56 curing

days [54]. Khatib and Hibbert et al. reported a significant flexural strength increase with up to 60 wt % GGBFS admixture; however, additional increases would adversely affect it [55]. Dejian Shen et al. investigated the residual tensile stress and the cracking potential of concrete and reported improvements to both parameters with up to 50 wt % GGBFS addition [56]. The beneficial effect of GGBFS was reported upon affecting the pore size, hence curtailing permeability [52]. Güneyisi et al. observed that only minute amounts typically less than 1000 Coulombs of charged chloride ion would be detected during the RCPT test when 20-50 wt % GGBFS was added to concrete. Others reported a 29 % reduction in passing electrical charge by adding up to 50 wt % GGBFS [57]. The diffusion coefficient of chloride in concrete also decreased with the addition of GGBFS [58, 59]. It has been observed that GGBFS can be effectively used to reduce the pore sizes and cumulative pore volume considerably, leading to more durable and impermeable concrete. According to the studies of Hwang and Lin, GGBFS has the potential to replace cement in high percentages because of its in-built cementitious property. The continued use of slag cement in the construction industry requires a consideration of the effect of electrochemically reducing pore solution on depassivation of steel reinforcement in cement system. Studies revealed that the inhibition of corrosion in slag concrete resulting from its low electrical conductivity caused a refined pore structure [48]. Nowadays, due to different environmental conditions, structures do not work as expected. Damage in the form of structural cracks due to stresses as well as scaling and shrinkage due to loss of fine aggregates and high wear, leakage, etc. lead to failure of concrete structures, and the use of ordinary concrete leads to premature destruction of structures. Therefore, the use of high-strength modified concrete as a building material in marine structures can be useful. The advantage of using such high performance concretes can reduce the cost of materials by reducing the thickness of the structure, increasing the mechanical, physical, and corrosion properties or saving the required materials. The use of GO in concrete is progressing due to its exceptional properties. Interest in GO has increased in various fields around the world because GO is more inexpensive than multi-walled CNTs, single-walled CNTs, and CNFs (which are 250, 1280, and 218 times more expensive than GO per 100 g, respectively) [60]. Therefore, GO became the best candidate for this research. This investigation was carried out to develop a nano-reinforced concrete composite in addition to GONP and GGBFS with varying percentages by weight of cement. No study has been reported on GO and GGBFS inclusion in concrete composites with regard to compressive strength, flexural strength, chloride permeation, and the cost analysis to get a clear picture whether this investigation is helpful for practical application in the construction industry. The present study focuses on the use of GONP-GGBFS as a nano-filler to develop a concrete for industrial applications in marine environment. The present research examines the effect of GONP and GGBFS addition on mechanical and permeability properties of concrete structures in marine environment. The optimized pozzolanic composition is achieved through the RSM optimization method to test this approach to designing a chlorine-resistant concrete for marine environments. The following are the specific objectives and scope of the present study:

- To study properties of concrete with the inclusion of GONP and GGBFS, thereby obtaining the mechanical performance of nano-modified concrete designed for industrial applications in marine environment;
- To determine the durability performance of nano-modified GONP-GGBFS based concrete mixes;
- To study the microstructural behavior of selected GONP-GGBFS-based concrete mixes through SEM and XRD analyses.

2. EXPERIMENTAL

2.1. Meterials

Type-II Portland cement with the chemical composition of Table 1 and the mechanical properties of the cement mortar in Table 2, measured per ASTM C109, was used. The sand and gravel gradation per ASTM C136 and ASTM C117 is shown in Tables 3 and 4. The GGBFS was procured from local sources with Blaine fineness of 3500 cm^2g^{-1}. The CaO/SiO_2 ratio was 1.4 based on the semi quantitative XRD (Figure 1) and XRF analysis (Table 5) corresponding to ASTM E1621-13. The water-to-cement ratio (W/C) was kept at 0.4. The FE-SEM microstructure images of nanoplatelets are shown in Figure 2, according to which the particle length varies from 2 μm to 15 μm and the average thickness is 7.7 nm. The FE-SEM images show the morphology of graphene oxide nano-sheets to be wrinkled thin lamellar layers interlinked to form a three-dimensional porous structure [21, 61, 62]. According to previous studies [22, 63-66], the inter-planar distance in the crystalline GO structure could be calculated from XRD pattern using Bragg's law: $\lambda = 2d\sin(\theta)$, where λ is the X-ray beam wavelength (in this case, $\lambda = 1.54$ A˚), d the distance between adjacent layers, θ the diffraction angle. According to XRD analysis in Figures 3 and 4, $d = \lambda/2 \sin(\theta) = 1.54$ A˚ / $2\sin(\theta)$ which would come to 6.8 Å for the initial sharp peak. The elemental analysis and physical properties of the GO are shown in Tables 6 and 7.

Table 1. The chemical analysis and hydration times of type-II cement according to ASTM C114 and ASTM C191

Constituent	%
SiO_2	21
Al_2O_3	4.5
Fe_2O_3	4
CaO	65.6
MgO	2.3
NaO	0.25
KO	0.41
Alkaline equivalent	0.52
SO_3	1.2
Cl	0.02
Insoluble residue	0.2
$3CaO.SiO_2$	66.9
$2CaO.SiO_2$	9.8
$3CaO{\cdot}Al_2O_3$	6.2
$4CaO.Al_2O_3.Fe_2O_3$	12.2
Initial hydration time (min)	104
Final hydration time (min)	225

Table 2. Compressive strength of portland type-II cements mortar according to ASTM C109

Age (days)	Compressive strength ($N.mm^{-2}$)
3	20.60
7	23.40
28	25.86
90	31.03

Table 3. Gradation of sand per ASTM C106 and ASTM C117

Square mesh size (mm)	Sieve number	Cumulative percentage of remained sand on the sieve (%)
9.500	3.8	0.0
4.750	4.0	9.6
2.360	8.0	35.3
1.180	16.0	58.0
0.600	30.0	75.0
0.300	50.0	84.9
0.150	100.0	95.1
0.075	200.0	97.7

Table 4. Gradation of gravel per ASTM C106 and ASTM C117

Square mesh size (mm)	Sieve number	Cumulative percentage of remained oval gravel on the sieve (%)	Cumulative percentage of remained pea gravel on the sieve (%)
50.00	2	0.0	0.0
37.50	1.5	0.0	0.0
25.00	1	0.0	0.0
19.00	3.4	5.3	0.0
12.50	1.2	65.7	31.3
9.50	3.8	93.6	62.8
4.75	4	99.9	99.6
2.36	8	99.9	99.9

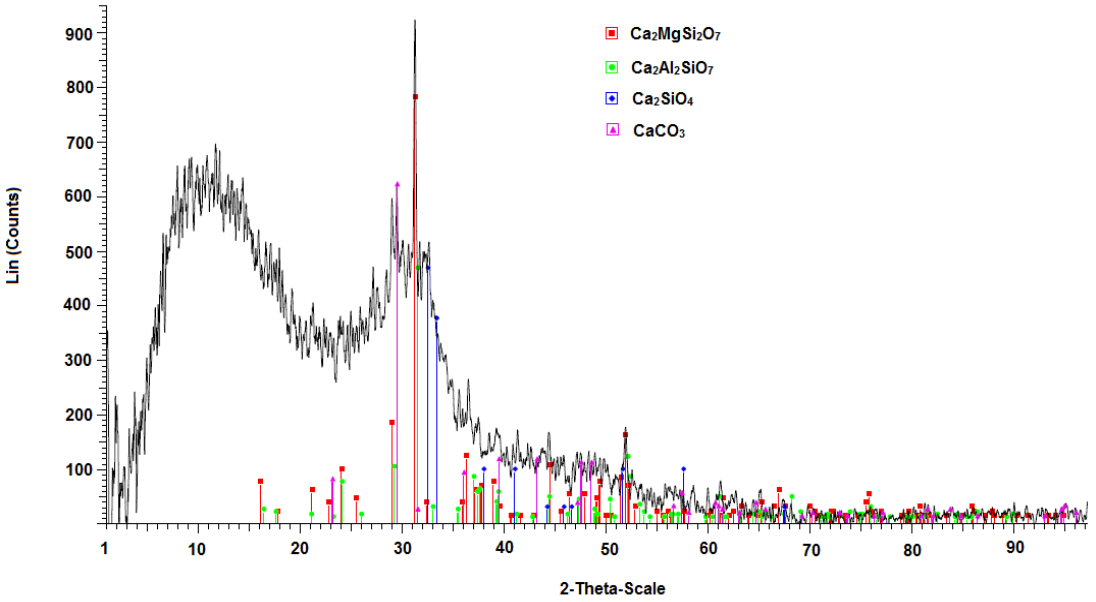

Figure 1. XRD analysis of GGBFS

Table 5. XRF and XRD chemical analysis results of GGBFS

Constituent	wt %
Na_2O	0.55
P_2O_5	0.06
CaO	43.64
SrO	0.18
MgO	6.17
S	1.25
TiO_2	1.81
BaO	0.32
Al_2O_3	9.16
Cl	0.02
MnO	1.96
L.O.I	1.50
SiO_2	31.10
K_2O	1.11
Fe_2O_3	1.17
TOTAL SUM	100.00

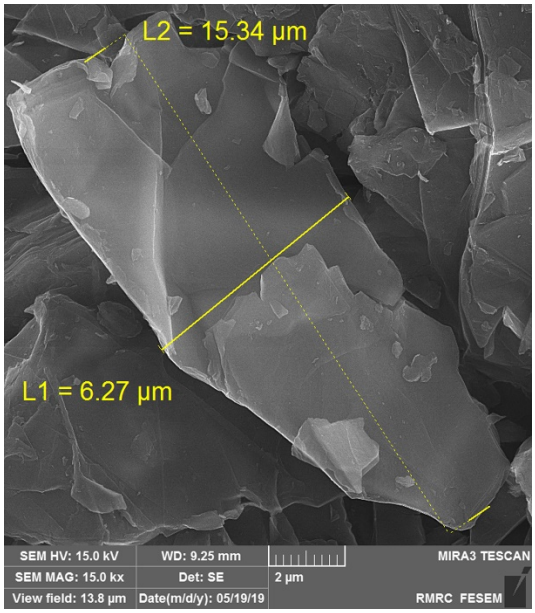

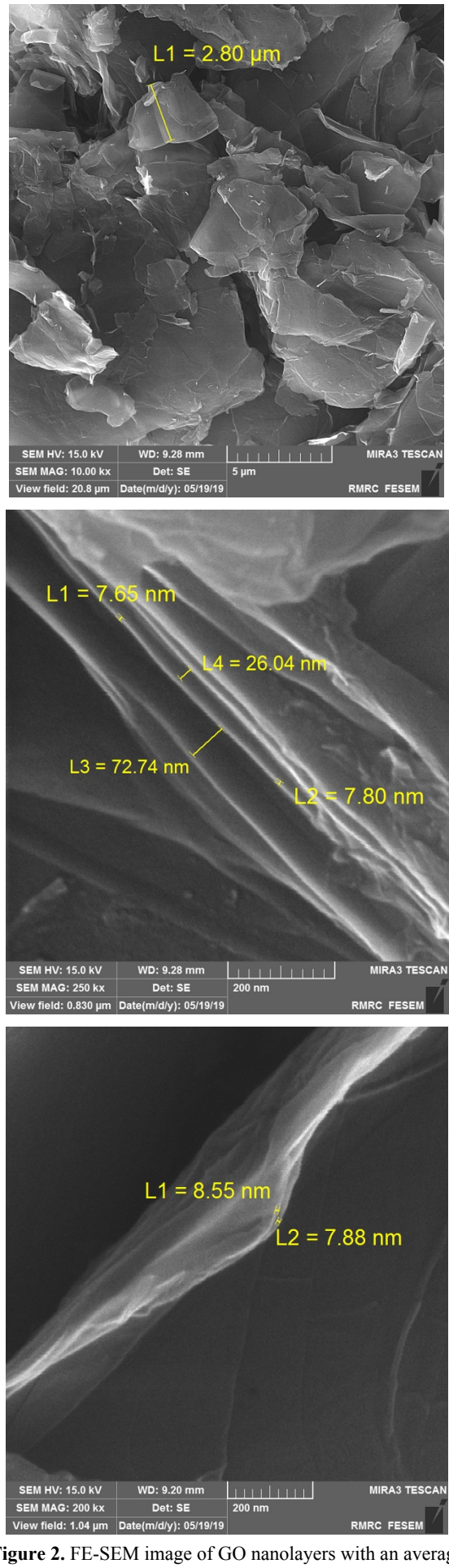

Figure 2. FE-SEM image of GO nanolayers with an average thickness of about 7.7 nm

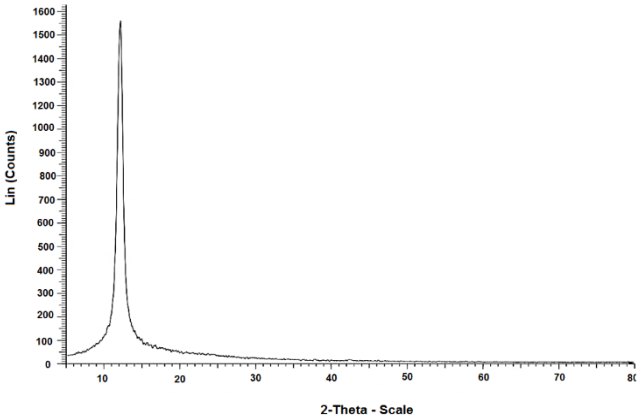

Figure 3. XRD analysis of dry GO before dispersion in water

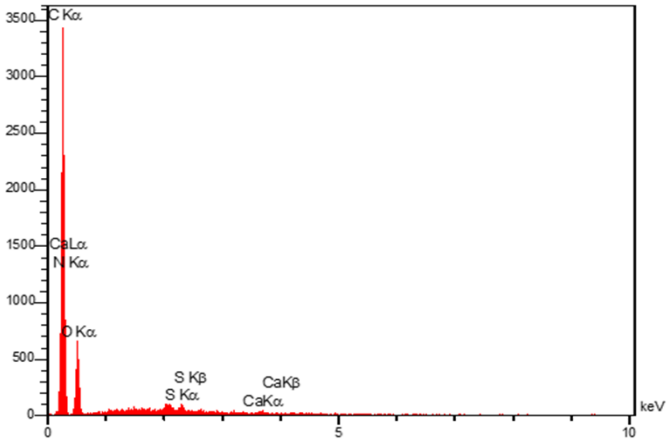

Figure 4. EDS area elemental analysis of GONP

Table 6. Elemental EDS analysis of graphene oxide nanoparticles

Element	C	N	O	S	Ca
%	70.87	0.88	27.81	0.28	0.16

Table 7. Physical properties of commercially procured GONP

Purity (%)	Size (µm)	Platelet thickness(nm)	No. of layers	Original packaged form
> 99	2-16	7.5-8.5	5-8	Black powder

2.2. Mortar mixing and curing procedure

Concrete mixes with compositions shown in Table 8 containing 30, 40, and 50 wt % of GGBFS and 0.01, 0.05, and 0.1 wt % of GONP were prepared. The GO solution for each mixing design was prepared according to the following:

1. For 0.01 wt % GO mix; 0.85 g of GO powder was added to 170 g water and 42.5 g polycarboxylate as a super plasticizer;
2. For 0.05 wt % GO mix; the total needed amount of GO powder (4.25 g) was divided into two equal parts and each was added to 508gr water and 21.25 g polycarboxylate,
3. For 0.1 wt % GO mix; the total amount of GO powder (8.5 g) was divided into three equal parts and each was added to 691.3 g water and 14.16 g polycarboxylate.

The weight percentage of GO was kept at 0.4 % in all solutions so as to homogenize them. The total dispersion is

achieved through sonication using a 300W and 20 kHz frequency transducer for 30 minutes. The graphene oxide solution and cement and aggregates mortar were mixed in a shear mixer for 3 minutes followed by 30 seconds on a shaker. The W/C ratio was kept constant by adding just the difference between the total water required and the water used to make the GO solution. ASTM C192M-16 standard was followed to make samples, which were kept in the molds in laboratory conditions for 24 hours and then, cured for 28 and 90 days at 25 °C and relative humidity of > 95 % in a water bath containing Lime. Polycarboxylate was used as a Super Plasticizer and 0.5 % by weight of cement in all samples.

Table 8. Quantity of materials used in m^3 of concrete samples

MIX	GGBFS (wt %)	GO (wt %)	GGBFS (kg/ m^3)	GO (kg/m^3)	OPC (kg/m^3)	Water (kg/m^3)	Fine aggregate (kg/m^3)	Coarse aggregate (kg/m^3)	SP (kg/m^3)
C	0.00	0.00	0.0	0.0000	425	170	1005.5	676.5	0.0425
G1	0.00	0.01	0.0	0.0425	425	170	1005.5	676.5	0.0425
G2	0.00	0.05	0.0	0.2125	425	170	1005.5	676.5	0.0425
G3	0.00	0.10	0.0	0.4250	425	170	1005.5	676.5	0.0425
S1	30	0.00	127.5	0.0000	297.5	170	1005.5	676.5	0.0425
S2	40	0.00	170.0	0.0000	255	170	1005.5	676.5	0.0425
S3	50	0.00	212.5	0.0000	212.5	170	1005.5	676.5	0.0425
SG1	30	0.01	127.5	0.0425	297.5	170	1005.5	676.5	0.0425
SG2	30	0.05	127.5	0.2125	297.5	170	1005.5	676.5	0.0425
SG3	30	0.10	127.5	0.4250	297.5	170	1005.5	676.5	0.0425
SG4	40	0.01	170.0	0.0425	255	170	1005.5	676.5	0.0425
SG5	40	0.05	170.0	0.2125	255	170	1005.5	676.5	0.0425
SG6	40	0.10	170.0	0.4250	255	170	1005.5	676.5	0.0425
SG7	50	0.01	212.5	0.0425	212.5	170	1005.5	676.5	0.0425
SG8	50	0.05	212.5	0.2125	212.5	170	1005.5	676.5	0.0425
SG9	50	0.10	212.5	0.4250	212.5	170	1005.5	676.5	0.0425

 OPC - Ordinary Portland Cement, GO – Graphene Oxide, GGBFS – Ground Granulated Blast Furnace Slag, SP – (Carboxylate based) Super Plasticizer

3. METHOD

3.1. Mechanical tests

ASTM C39M-18 and C78M-18 standard tests were followed for examining the compression and flexural strength of concrete specimens.

3.2. Resistance to chlorine permeation test (RCPT)

Chloride permeability resistance was evaluated per ASTM C1202 accelerated test on cylindrical samples with 10 cm diameter and 5 cm length made specifically for the test. An electrical current passed through the concrete sample under a constant 60 V DC potential difference for six hours on the one side and was measured on the other side. One end was immersed in 3 % sodium chloride solution and the other in a 0.3 M solution of sodium hydroxide [67]. The total coulombs of electricity passed, becoming proportional to the electrical resistance of the specimen which inversely relates to chloride ion penetrating the sample. Therefore, the lower the electric current, the higher the resistance to chloride ingress.

3.3. Electrical resistivity of concrete

Wenner's four-point line array test is a well-established technique for measuring the resistivity of soil and semiconducting materials. For determining the resistivity of concrete, this test is applied with modifications based on AASTHO TP 95-11 standard. In a more common form, four equally spaced electrodes are arranged linearly to measure the electrical resistivity. The two outer electrodes apply an AC current to the concrete surface, while the electrical potential is measured between the inner probes. The electrodes in a four-probe square array are arranged in a square position at 50 to 100 mm spacing [68, 69].

3.4. Response surface optimization and statistical analysis

The selection of the optimal concrete composition in terms of the highest electrical resistance and mechanical properties was done by Response Surface Method (RSM). The experimental data were the required input for the Design-Expert software version 7.0.1.0 and a Central Composite Face centered Design (CCFD) comprising technique was employed. The variables considered in the optimization were the weight percentages of graphene oxide and granulated blast furnace slag, whereas the response variables were the compressive strength, flexural strength, RCPT data, and electrical resistance. The software assigns the required number of experiments based on the number of variables (Percentages of GGBFS and GO) and responses measured (RCPT, Electrical resistance, compressive strength, and Flexural strength) which comes to 10 runs (Table 9).The experimental data were fitted to a polynomial model of quadratic equations and the optimization software performed an analysis for determining the best combination of maximum mechanical properties and electrical resistivity and the lowest RCPT possible. For each response, a function that related it to the two variables of weight percentages of graphene oxide and ground granulated slag was determined (Table 10). Finally, a goal function was determined that gave the general desirability of the combined four different responses.

4. RESULTS AND DISCUSSION

4.1. Mechanical properties

Figures 5 and 6 show the results of mechanical tests for samples following 28 and 90 curing days demonstrating the marginal enhancement of mechanical properties, mainly in G1, G2, S1, SG1, and SG3 mixes.

Table 9. The designed experimental runs as fed to the software modified for higher accuracy

Run No.	A (GGBFS) (wt %)/100	B(GO) (wt %)/100	Compressive strength (R1)	Flexural strength (R2)	RCPT (R3)	Electrical resistivity (R4)
1	0	0.0000	28.4	2.2	7008.46	14
2	0.40	0.0000	33	2.4	4352.14	38.1
3	0.50	0.0000	34.1	2.3	3788.19	49
4	0.30	0.0005	32.4	2.9	7702.52	36.6
5	0.30	0.0010	35.1	2.9	4250.64	28.9
6	0.40	0.0005	33.7	2.6	3766.93	36.3
7	0.40	0.0010	33.8	2.5	2428.01	36.8
8	0.50	0.0005	34.4	2.5	3460.95	45.6
9	0.50	0.0010	33.4	2.6	2058.18	40.8
10	0	0.0010	32.9	2.8	5862.41	12.4

Table 10. The models selected for each response (variables are A: GGBFS wt % and B: GO wt %)

Response	Model	Final equations for each response	R^2
Compressive strength (R1)	Quadratic	R1=+28.22493+16.35659 * A +4444.14506* B -10071.42857 *A* B -9.50178* A^2+4.33096E+005 * B^2	0.9273
Flexural strength (R2)	Quadratic	R2=+2.21221+1.89760 * A +1164.36197* B -785.71429 * A * B -3.52313 * A^2 5.69751E+005 * B^2	0.8515
RCPT (R3)	Quadratic	R3 =+7096.35542 +528.13747 *A +3.71687E+006 * B -1.39000E+006* A * B -16135.60973 * A^2 - 4.88790E +009 * B^2	0.8388
Electrical resistivity (R4)	Quadratic	R4= +13.91885 +64.69156* A + 5545.50359 * B -9214.28571 * A * B+2.73428* A^2-6.72432E+006* B^2	0.9755

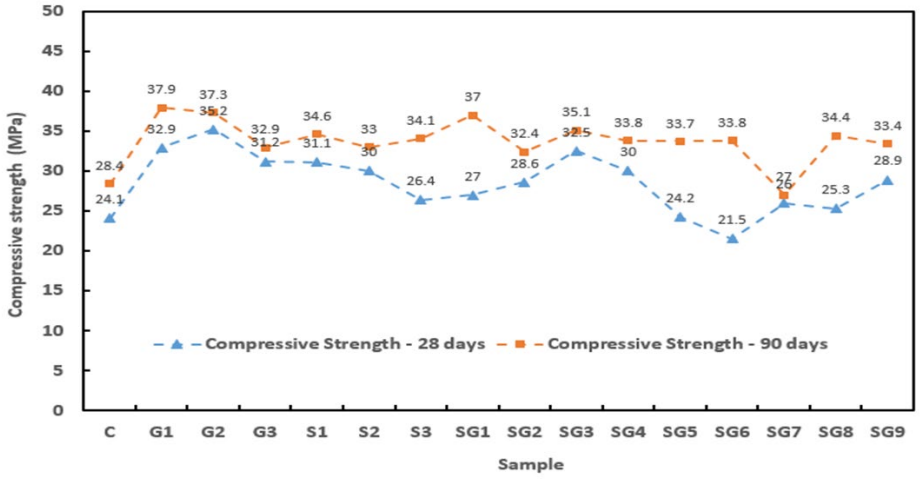

Figure 5. Compressive strength of concrete samples on 28 and 90 days (curing time)

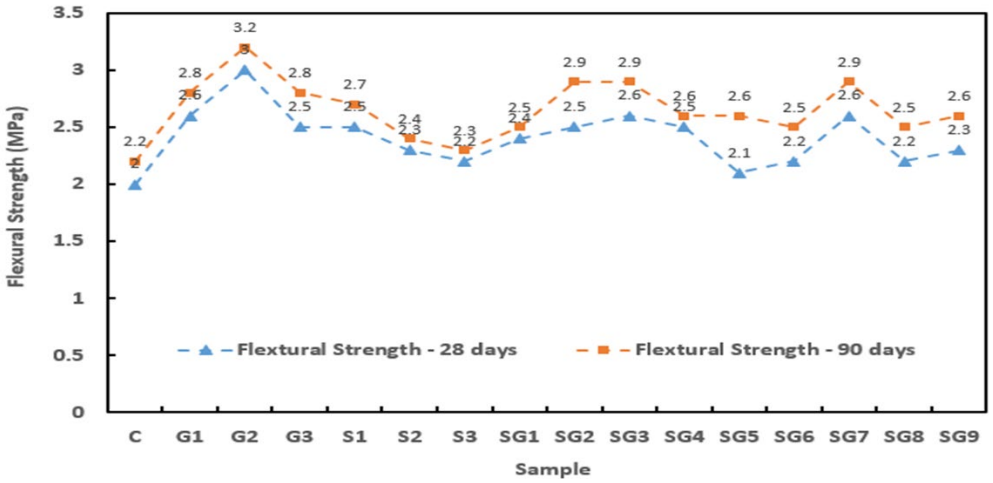

Figure 6. Flextural strength of concrete samples on 28 and 90 days (curing time)

These results show that the addition of 30 wt % GGBFS in GO-free concrete samples resulted in 21.8 % and 29.0 % increases in compressive strength at curing time 28-days and 90-days, respectively. Literature reports indicate that increasing the GGBFS content delays the curing time of concrete to reach maximum strength [56-59, 70, 71]. This is because of the slow calcium hydroxide-dependent pozzolanic reaction of GGBFS (Eq.1):

$$CaOH_2CH+SiO_2S+H_2O=CSH\text{-}gel \quad (1)$$

As the Portland cement gradually hardens by forming phases such as allite and billet, calcium hydroxide is released, which leaches out and deteriorates concrete. When GGBFS is added to the cement mixture, the hydrated calcium silicate is formed instead by the direct interaction of calcium hydroxide and GGBFS [71]. This is a good adhesive and results in improved mechanical properties.

Figure 7 shows the effect of GONP and GGBFS individually on compressive strength. While additions below 30 wt % GGBFS to GONP-free concrete have good effect on mechanical properties (Figure 7b), any addition above that is not beneficial either and may lower the compressive strength. For example, a 17.8 % reduction in compressive strength on Day 28 (curing time) was observed by increasing GGBFS from 30 wt % to 50 wt %. in GONP-free samples. However, in this study, some cases even after admixes of up to 40 wt % did not exhibit significant reductions in compressive strength compared to the 30 wt % case. For instance, following 28 days curing of 0.01 wt % GONP-40 wt % GGBFS concrete mixes (SG4), the compressive strength increased by approximately 11 % compared to 0.01 wt % GONP-30 wt % GGBFS (SG1); however, for most mixtures containing GGBFS and GONP, admixing only 30 wt % GGBFS with varying amounts of GONP was enough for achieving high levels of compressive strength. This is true for 28- and 90-day cured samples (SG3) and 90-day cured (SG1) samples; this finding is in good agreement with the published literature [54, 72]. A reduction by nearly 11.7 % of compressive strength after 28 days of curing is reported when 50 wt % GGBFS is added [54], although the 0.05 wt % GONP-50 wt % GGBFS samples (SG8) cured for 90 days exhibited a 6 % increase in the compressive strength as compared to 0.05 wt % GONP-30 wt % GGBFS (SG2). In the GONP and GGBFS mixes, the effect of GONP addition on mechanical properties exhibited an uncertain trend. For example, in 30 wt % GGBFS samples, the addition between 0.01 and 0.1 % GONP improved the 28-day compressive and flexural strength by 20.37 % and 8.33 %, respectively; however, the GONP addition to 40 % GGBFS samples lowered compressive strength.

Overall, based on the reports by other researchers, it can be concluded that the discrepancies in the mechanical strength observed at shorter curing times do not warrant changing the limit for the best weight percentage of GGBFS [54, 73]. Therefore, if only mechanical strength is aimed at, a 30 wt % GGBFS addition is enough to get the desired increase in compressive strength. In the GGBFS-free samples, the addition of 0.05 wt % of GONP resulted in 30-40 % improvement in compressive strength after 28 and 90 curing days; however, this declines when over 0.05 % GONP is used (Figure 7a).

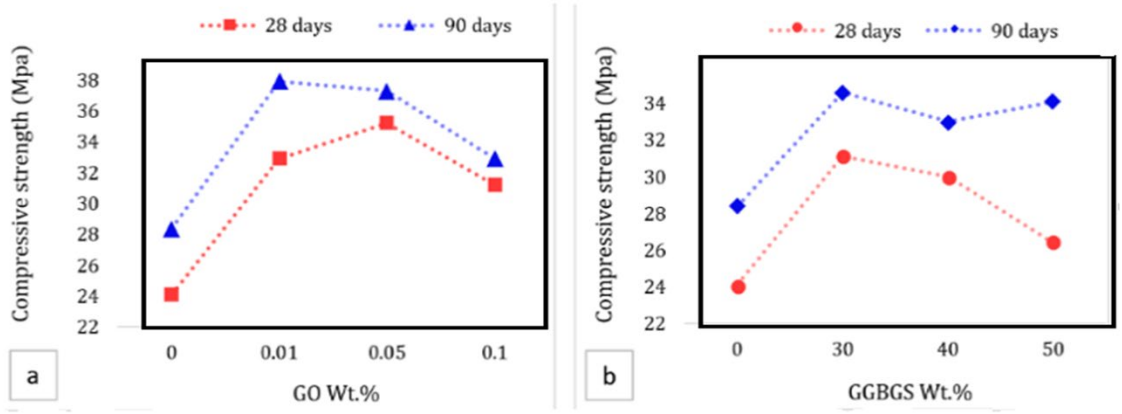

Figure 7. The effect of (a) GONP and (b)GGBFS individually on compressive strength

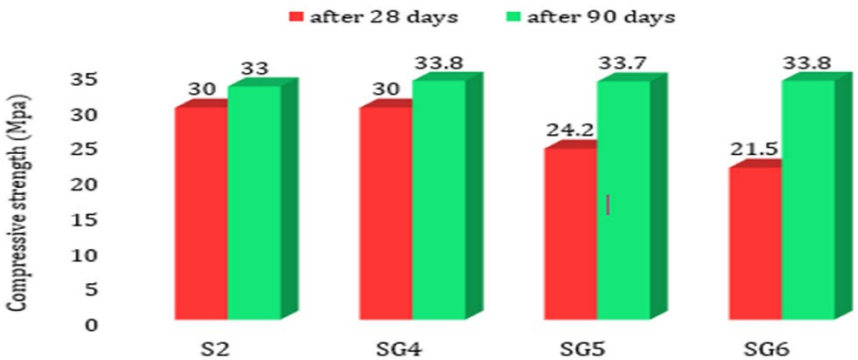

Figure 8. The compressive strength of 40 wt % GGBFS-containing samples with different GO additions

Figure 8 shows the changes in compressive strength upon increasing GONP content in 28- and 90-day cured samples (S2), (SG4), (SG5), and (SG6). Overall, higher graphene oxide content leads to a delay in gaining strength. An increase

in the compressive strength of the GONP-containing concretes with curing time was reported and in the present work, the highest mechanical strengths were obtained for the G1, G2, and SG1 samples following 90 curing days (Table 11).

Table 11. The highest mechanical results for different mixes on 90 days (curing time)

Sample code	Compressive strength (MPa)	Flexural strength (MPa)	Improvement (%)
G1	37.9	2.8	33.4
G2	37.3	3.2	31.3
SG1	37.0	2.5	30.2

GONP's impact is more pronounced in GGBFS free samples [74]. Increases of 15-48 % in compressive strength have been reported for 0.05 wt % graphene oxide addition [17, 33, 36]. Mao Li et al. observed a 16 % decrease in compressive strength when 0.05 % GO was added in the presence of 25 % GGBFS [75]. In the current study, the maximum compressive strength was measured for the 28- and 90-day cured samples with 0.05 % GO, showing 46 % (35.2 MPa) and 31 % (37.3 MPa) improvements, respectively. The strength-giving property of graphene oxide depends to a large extent on the quality of its production, its purity, and its proper dispersion in the concrete mix, which has given rise to the scatter seen in the results seen in some studies [22].

4.2. Wenner test and RCPT results

Free chloride is known for fast diffusion into concrete, but GGBFS in concrete may reduce this using the chloride binding capacity of concrete [76-79]. Figures 9 and 10 show Wenner test and RCPT results for 28- and 90-day cured samples, respectively.

Figure 9 shows the Wenner test results from SG9 samples (0.1 wt % GONP and 50 wt % GGBFS), exhibiting high surface electrical resistivity and the least electrical charge conduction (1200 to 2058 C), a sign of high resistance to chloride ingress. The observation that the addition of GGBFS in 28- and 90-day cured samples significantly decreases the charge conducted in RCPT tests points to the increased resistance against chloride penetration.

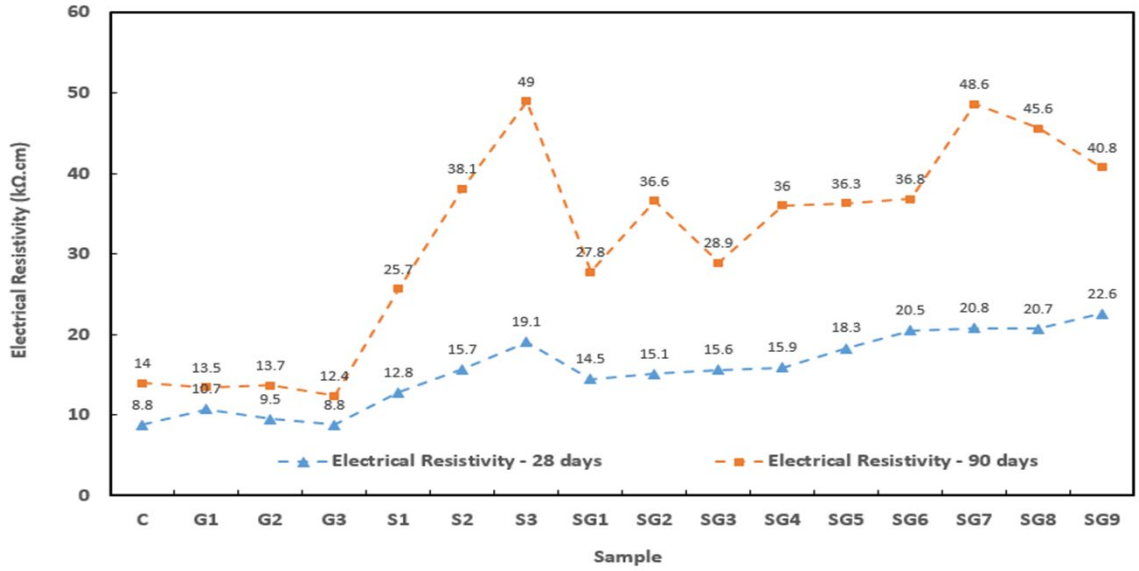

Figure 9. The Wenner test results of 28- and 90-day cured concrete samples

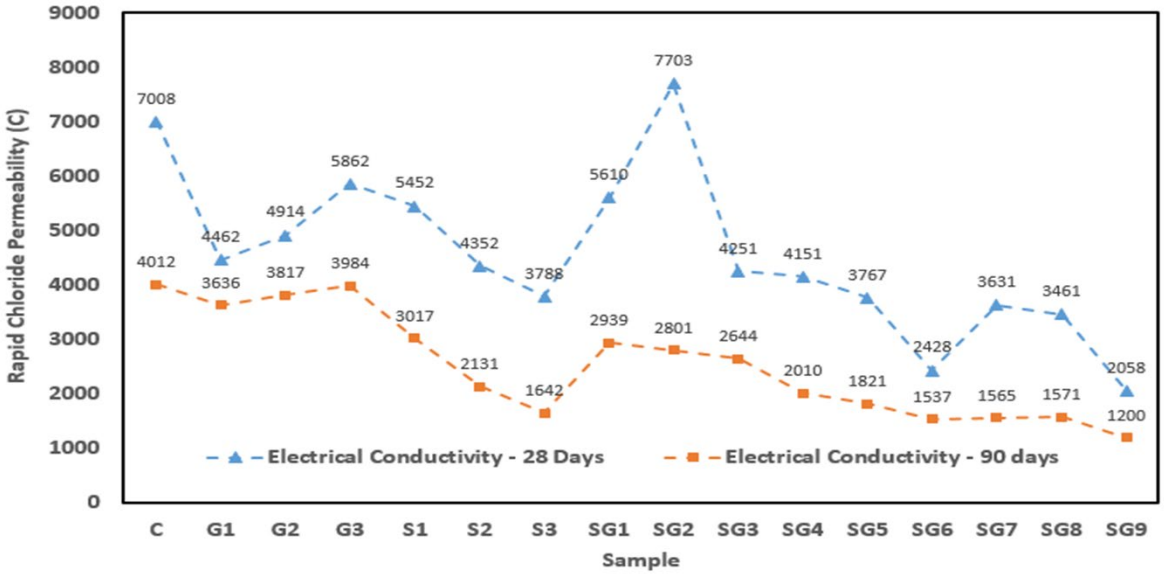

Figure 10. The RCPT test results of 28- snd 90-day cured concrete samples

The ASTM 1202-12 Standard [67] designates such charge conduction as low chloride permeability (Table 12). Maochieh et al. reported conducted currents following 91 days of curing for 40 wt % and 60 wt % GGBFS concretes as 1394 C and 1883 C, respectively, while other published papers exhibited conduction in the region of 1659.6 C [58, 59].

Table 12. Chloride ion penetrability based on charge passed according to ASTM 1202-12 Standard [67]

The charge passed (C)	Chloride ion permeability
>4000	High
2000-4000	Moderate
1000-2000	Low
100-1000	Very low
<100	Negligible

Electrical charge transfer during the RCPT test significantly declines in the concrete containing higher GGBFS content, confirming the positive role of GGBFS in decreasing the chloride permeability and movement by immobilizing the free chloride. In our study, the 28-day 30 wt % GGBFS concrete passed nearly 5452 C and after 90 days, it conducted 3017 C which is desirable in terms of chloride permeability. In the current study, the addition of GONP to ordinary concrete increased the conductivity and decreased electrical resistance, although for G1 (0.01 wt % GONP), a reduction of nearly 9.3 % in electrical conductivity was observed. The highest electrical resistivity was achieved (49 kΩ.cm) for 90-day cured samples with 50 % GGBFS. Maochieh reports the electrical resistivity of the 90-day cured 60 wt % GGBFS concerts as 34.8 kΩ.cm [80]. Overall, GONP in GGBFS free concrete did not have a positive effect on chloride permeability. According to results from Figures 9 and 10, the lowest charge was passed when concretes contained GGBFS and GONP. For example, the addition of 0.1 wt % GONP with 50 wt % GGBFS reduced the passing charge from 1642 C to 1200 C. A significant reduction in electrical conductivity from 4012 C to 1200 C was observed for 90-day cured samples containing 0.1 wt % GO-50 wt % GGBFS (SG9) compared to the control sample. Based on these results, the addition of 0.1 wt % GO and 50 wt % GGBFS could effectively reduce the passing current in the conductivity test and enhance the resistance of concrete to chloride penetration. Figure 11 shows the effect of GONP and GGBFS individually on Wenner test and RCPT.

Addition of GONP to conventional concrete increased the conductivity and decreased electrical resistance, although for G1 (0.01 wt % GONP), a reduction of nearly 9.3 % in electrical conductivity was observed. The highest electrical resistivity was achieved (49 kΩ.cm) for 90-day cured samples with 50 % GGBFS and 0.1 % GONP to be highly effective in increasing concrete resistance to chloride penetration.

The values of electrical conductivity for admixture were obtained by other researchers in the same condition are shown in Table 13 [23, 35-48], proving that the chloride ion penetrability value for 90-day cured samples containing 0.1 wt % GO-50 wt % GGBFS (SG9) is low and this mix has good resistance to chlorine ion permeability compared to other admixtures.

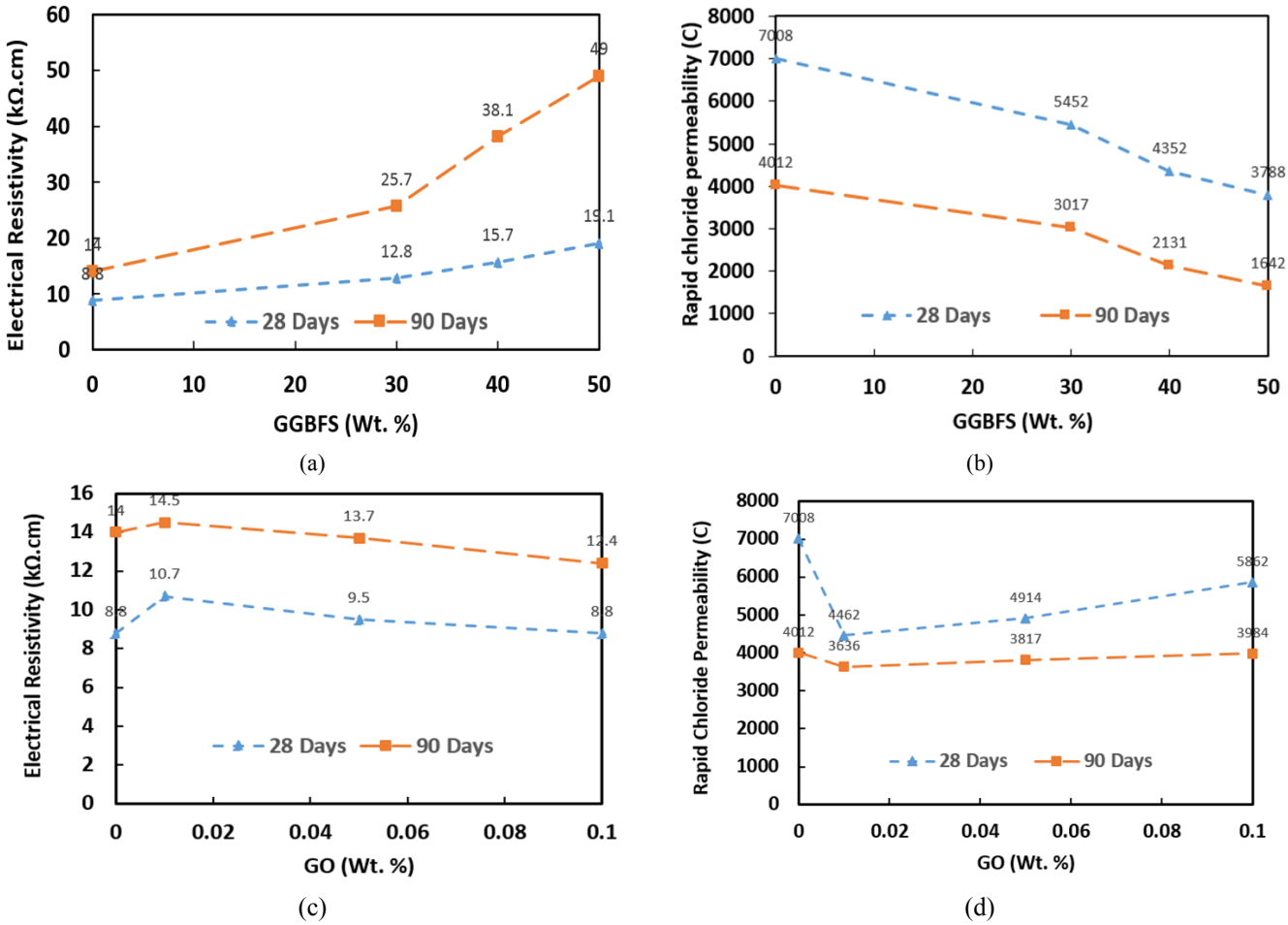

Figure 11. The effect of (a,b) GGBFS and (c,d) GONP individually on electrical resistance and electrical conductivity

Table 13. The charge passed values for admixtures obtained from some other studies and this research

Mix	The charge passed (C)	Reference
5 wt % Silica Fume	850	[72]
30 wt % Fly Ash	2000	[81]
50 wt % Fly Ash	2550	[81]
30 wt % GGBFS	1750	[81]
40 wt % GGBFS	1394	[72]
40 wt % GGBFS	6300	[82]
50 wt % GGBFS	1340	[81]
50 wt % GGBFS	1600	[72]
60 wt % GGBFS	1883	[72]
60 wt % GGBFS	3000	[82]
0.03 wt %GO	1630	[83]
0.06 wt %GO	1530	[83]
0.09 wt %GO	1560	[83]
0.1 wt % GO-50 wt % GGBFS	1200	This paper

4.3. Cost analysis

The cost of casting the mixed designed was analyzed, as reported in Tables 14 and 15. The cost of concrete composites was evaluated using the commercialized market prices of the materials. The economic Index for strength (compressive strength/cost per m^3) was observed to have the maximum value at the mix G1 (with 0.01 % GO inclusion) compared to the rest of the mixes and the economic index for electrical conductivity (electrical conductivity/cost per m^3) shows that the mix SG9 is a better mix than the rest in terms of chlorine ion permeability and economy. Table 15 shows that the cost of materials for making SG9 sample is 24.5 % higher than that of conventional concrete; however, considering economic index for electrical conductivity, use of this mix is cost-effective. According to this table, the value of this index for SG9 decreased by more than 4 times compared to that for the conventional concrete.

Table 14. Cost of materials

Materials	Cost (USD/kg)
OPC	0.1
GO	16.32
GGBFS	0.15
Water	0.0007
Fine aggregate	0.02
Coarse aggregate	0.013
SP	1.6

 OPC - Ordinary Portland Cement, GO – Graphene Oxide, GGBFS – Ground Granulated Blast Furnace Slag, SP – (Carboxylate based) Super Plasticizer

4.4. Optimization results

The levels of the priority given to the responses were RCPT (high), Electrical resistance (high), compressive strength (moderate), and Flexural strength (low). By feeding the experimental data from the mechanical, RCPT, and the Wener tests to the response surface method software, the relation between each response and GONP and GGBFS alterations was modeled, as shown in Figure 12. Optimization results helped predict that 0.08 wt % GO and 50 wt % GGBFS and 90-day curing led to the most desirable mechanical and physical properties with a remarkable improvement in chlorine ingress resistance. This was shown to be in good agreement with the actual results from real-world experiments. The desirability level of this composition based on the criteria specified for the software was calculated as 0.831 (Figure 13).

Table 15. Cost analysis of different mixes per m^3 of concrete

Mix	Cost (USD)								Properties		Economic index	
	GGBFS	GO	OPC	Water	FA	CA	SP	Total cost	CS	EC	EI_1	EI_2
C	0	0	42.5	0.119	20.11	8.794	0.068	71.591	28.4	4012	0.397	56.040
G1	0	0.694	42.5	0.119	20.11	8.794	0.068	72.285	37.9	3636	0.524	50.300
G2	0	3.468	42.5	0.119	20.11	8.794	0.068	75.059	37.3	3817	0.497	50.853
G3	0	6.936	42.5	0.119	20.11	8.794	0.068	78.527	32.9	3984	0.418	50.733
S1	19.125	0	29.75	0.119	20.11	8.794	0.068	77.966	34.6	3017	0.444	38.696
S2	25.5	0	25.5	0.119	20.11	8.794	0.068	80.091	33	2131	0.412	26.607
S3	31.875	0	21.25	0.119	20.11	8.794	0.068	82.216	34.1	1642	0.415	19.971
SG1	19.125	0.694	29.75	0.119	20.11	8.794	0.068	78.6601	37	2939	0.470	37.363
SG2	19.125	3.468	29.75	0.119	20.11	8.794	0.068	81.434	32.4	2801	0.398	34.395
SG3	19.125	6.936	29.75	0.119	20.11	8.794	0.068	84.902	35.1	2644	0.413	31.142
SG4	25.5	0.694	25.5	0.119	20.11	8.794	0.068	80.785	33.8	2010	0.418	24.881
SG5	25.5	3.468	25.5	0.119	20.11	8.794	0.068	83.559	33.7	1821	0.403	21.793
SG6	25.5	6.936	25.5	0.119	20.11	8.794	0.068	87.027	33.8	1537	0.388	17.661
SG7	31.875	0.694	21.25	0.119	20.11	8.794	0.068	82.910	27	1565	0.325	18.876
SG8	31.875	3.468	21.25	0.119	20.11	8.794	0.068	85.684	34.4	1571	0.401	18.335
SG9	31.875	6.936	21.25	0.119	20.11	8.794	0.068	89.152	33.4	1200	0.375	13.460

 OPC - Ordinary Portland Cement, GO – Graphene Oxide, GGBFS – Ground Granulated Blast Furnace Slag, FA - Fine Aggregate, CA - Coarse Aggregate, SP – (Carboxylate based) Super Plasticizer, CS – Compressive Strength, EC – Electrical Conductivity, EI1- The economic Index for Strength, EI2 - The economic Index for electrical conductivity

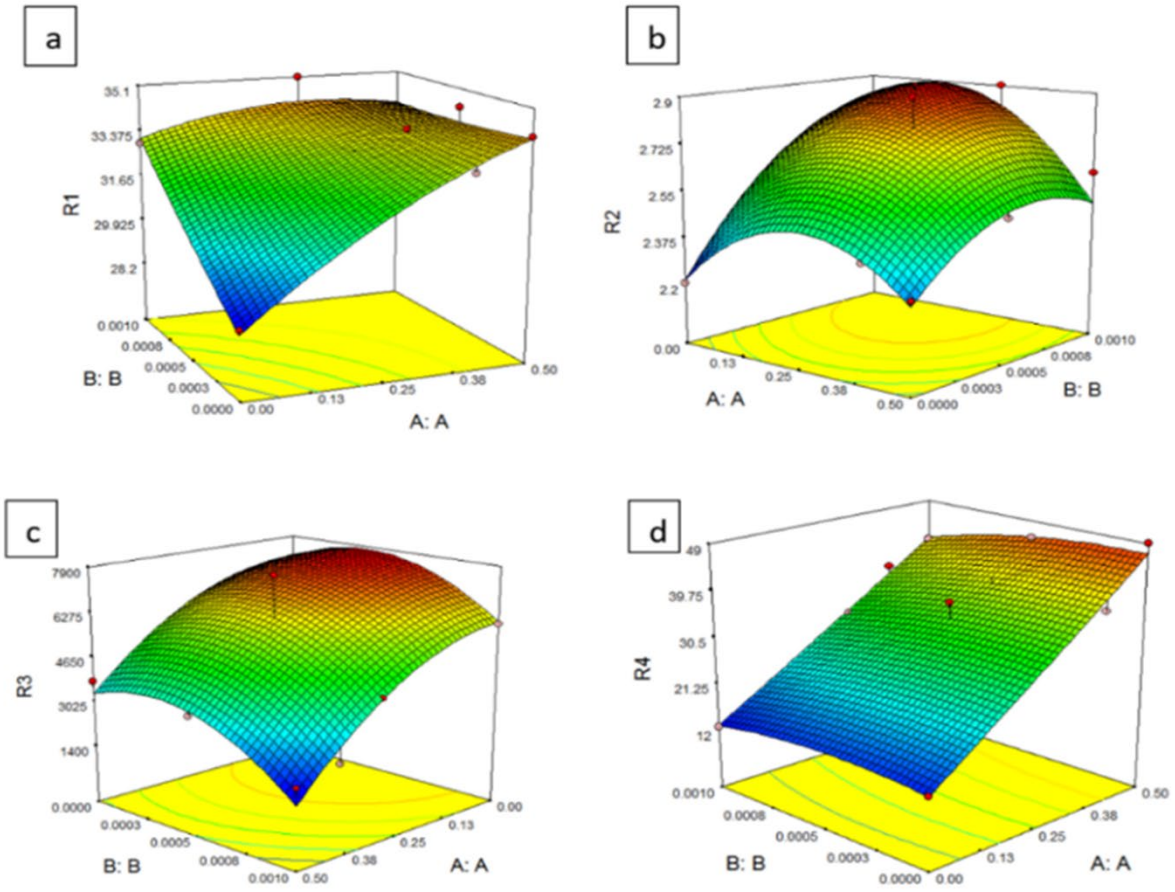

Figure 12. The effect of GO and GGBFS variation on (a) compressive strength, (b) flexural strength, (c) RCPT results, and (d) surface electrical resistivity

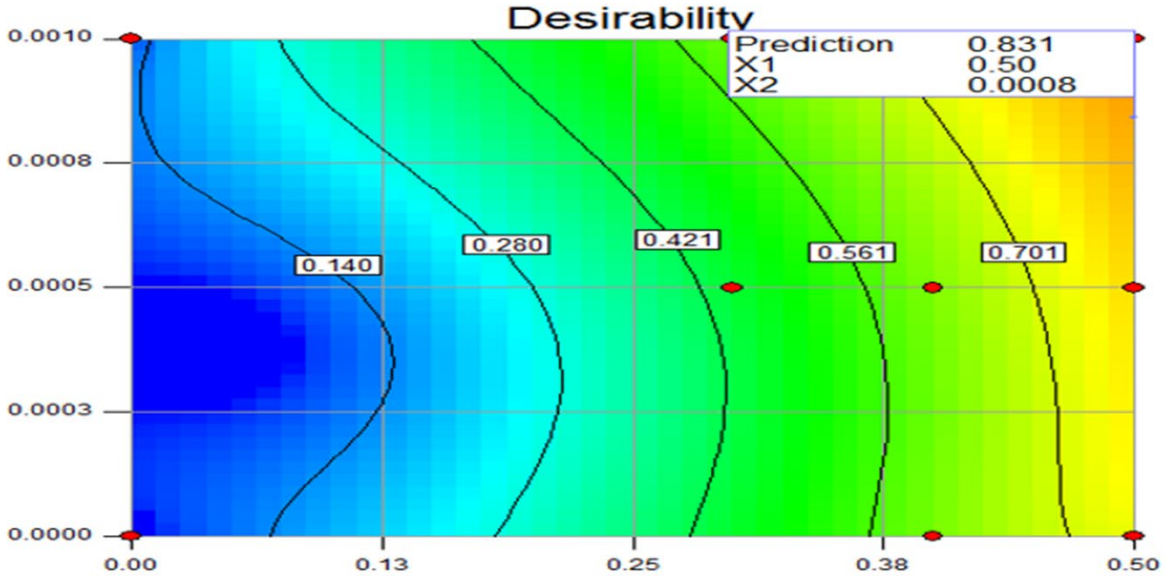

Figure 13. Desirability contour of different compositions and the selected final mixture

5. CONCLUSIONS

- The addition of slag up to 30 % by weight was effective in improving the compressive and flexural strength of graphene oxide-free specimens; however, addition of more than 30 % by weight could even reduce the compressive and flexural strength of concrete specimens. Therefore, the addition of 30 wt % GGBFS to concrete after 90 days resulted in the highest mechanical properties; however, to improve the resistance against chloride penetration, this should be increased to 50 wt %, thus forfeiting some mechanical strength.
- Prolonging the curing duration in concrete samples with GONP and GGBFS is essential to achieving higher levels of mechanical properties.

- GGBFS had a more pronounced role than GONP in developing the concrete resistance against chloride penetration.
- In the GGBFS-free samples, addition of 0.05 wt % of GONP yielded the improvement of compressive and flexural strength after 28 and 90 curing days; however, this strength declined when using over 0.05 % GONP.
- In the GGBFS-free samples, addition of 0.01 wt % of GONP was enough to achieve the highest chloride penetration resistance.
- Combined GONP and GGBFS additions enhanced the resistance to chloride permeation.
- The addition of 0.1 % graphene oxide and 50 % granular slag increased the compressive strength of concrete sample by 19.9% during 28 days and 17.6% during 90 days compared to the conventional concrete sample.
- Concrete with a combination of 0.1 % graphene oxide and 50 % granular slag caused an increase in flexural strength by 15 % during 28 days of curing and by 13.6 % during 90 days of curing.
- A high reduction in electrical conductivity from 4012 C to 1200 C was observed for 90-day cured samples containing 0.1 wt % GO and 50 wt % GGBFS compared to the conventional sample.
- In the GONP-free samples, the addition of 50 wt % GGBFS exhibited the highest surface electrical resistivity and the least electrical charge conduction, which is a sign of high resistance to chloride ingress.
- Based on experimental data, 0.1 wt % GONP and 50 wt % GGBFS admixtures in concrete were of optimal mixing in terms of chlorine ion penetration and corrosion resistance.
- From the cost analysis and the economic index calculated, the economic Index for Strength (compressive strength/cost per m^3) was observed to have maximum value at mix G1 (with 0.01 % GO inclusion) compared to the rest of the mixes and the economic Index for electrical conductivity (electrical conductivity/cost per m^3) showed that mix SG9 was the optimum mix.

Based on experimental data and optimization as well as statistical analysis, a concrete mix containing 0.08 wt % GONP and 50 wt % GGBFS combined high mechanical properties and excellent resistance against chloride ions permeation.

6. ACKNOWLEDGEMENT

The authors appreciatively acknowledge the Research Council of Shahid Bahonar University.

REFERENCES

1. Li, W., Dong, W., Tam, V.W.Y. and Yu, T., "Durability deterioration of concrete under marine environment from material to structure: A critical review", ***Journal of Building Engineering***, Vol. 35, (2021), 1-17. (https://doi.org/10.1016/j.jobe.2020.102074).
2. James, A., Bazarchi, E., Chiniforush, A., Aghdam, P., Hosseini, M.R., Akbarnezhad, A., Martek, I. and Ghodoosi, F., "Rebar corrosion detection, protection and rehabilitation of reinforced concrete structures in coastal environments: A review", ***Construction and Building Materials***, Vol. 224, (2019), 1026-1039. (https://doi.org/10.1016/j.conbuildmat.2019.07.250).
3. Fan, J., Zhu, H., Shi, J., Li, Z. and Yang, S., "Influence of slag content on the bond strength, chloride penetration resistance, and interface phase evolution of concrete repaired with alkali activated slag/fly ash", ***Construction and Building Materials***, Vol. 263, (2020), 1-9. (https://doi.org/10.1016/j.conbuildmat.2020.120639).
4. Ramezanianpour, A.A., Ghoreishian, S., Ahmadi, B., Balapour, M. and Ramezanianpour, A.M., "Modeling of chloride ions penetration in cracked concrete structures exposed to marine environments", ***Structural Concrete***, Vol. 19, (2018), 1460-1471. (https://doi.org/10.1002/suco.201700285).
5. Goyal, A., Olorunnipa, E.K., Sadeghi Pouya, H., Ganjian, E. and Olubanwo., A.O., "Potential and current distribution across different layers of reinforcement in reinforced concrete cathodic protection system- A numerical study", ***Construction and Building Materials***, Vol. 262, (2020), 1-10. (https://doi.org/10.1016/j.conbuildmat.2020.120580).
6. Bahekar, P.V. and Gadve, S.S., "Impressed current cathodic protection of rebar in concrete using carbon FRP laminate", ***Construction and Building Materials***, Vol. 156, (2017), 242-251. (https://doi.org/10.1016/j.conbuildmat.2017.08.145).
7. Du, F., Jin, Z., She, W., Xiong, C., Feng, G. and Fan, J., "Chloride ions migration and induced reinforcement corrosion in concrete with cracks: A comparative study of current acceleration and natural marine exposure", ***Construction and Building Materials***, Vol. 263, (2020), 1-11. (https://doi.org/10.1016/j.conbuildmat.2020.120099).
8. Rodrigues, R., Gaboreau, S., Gance, J., Ignatiadis, I. and Betelu, S., "Reinforced concrete structures: A review of corrosion mechanisms and advances in electrical methods for corrosion monitoring", ***Construction and Building Materials***, Vol. 269, (2021), 1-36. (https://doi.org/10.1016/j.conbuildmat.2020.121240).
9. Tuutti, K., Corrosion of steel in concrete: Cement-och betonginst, (1982). (https://lucris.lub.lu.se/ws/files/4709458/3173290.pdf).
10. Zhang, D. and Shao, Y., "Enhancing chloride corrosion resistance of precast reinforced concrete by carbonation curing", ***ACI Materials Journal***, Vol. 116, (2019), 3-12. (https://doi.org/10.14359/51714461).
11. Tang, L. and Nilsson, L., "Service life prediction for concrete structures under seawater by a numerical approach", ***The Durability of Building Materials and Components***, Vol. 7, (1996), 97-106. (https://jglobal.jst.go.jp/en/detail?JGLOBAL_ID=200902187425051487).
12. Jung, M.S., Kim, K.B., Lee, S.A. and Ann, K.Y., "Risk of chloride-induced corrosion of steel in SF concrete exposed to a chloride-bearing environment", ***Construction and Building Materials***, Vol. 166, (2018), 413-422. (https://doi.org/10.1016/j.conbuildmat.2018.01.168).
13. Stanish, K., Hooton, R.D. and Thomas, M.D., "Testing the chloride penetration resistance of concrete: A literature review", ***The United States Federal Highway Administration***, (2001). (https://www.researchgate.net/publication/237321599_Testing_the_Chloride_Penetration_Resistance_of_Concrete_A_Literature_Review).
14. Daniyal, M., Azam, A. and Akhtar, S., "Application of nanomaterials in civil engineering", Nanomaterials and Their Applications, Springer, Singapore, (2018), 169-189. (https://doi.org/10.1007/978-981-10-6214-8_6).
15. Sobolev, K. and Gutiérrez, M.F., "How nanotechnology can change the concrete world", ***American Ceramic Society Bulletin***, Vol. 84, (2005), 113-116. (https://doi.org/10.1002/9780470588260.ch17).
16. Chuah, S., Pan, Z., Sanjayan, J.G., Wang, C.M. and Duan, W.H., "Nano reinforced cement and concrete composites and new perspective from graphene oxide", ***Construction and Building Materials***, (2014). (https://doi.org/10.1016/j.conbuildmat.2014.09.040).
17. Pan, Z., He, L., Qiu, L., Korayem, AH., Li, G. and Zhu, J.W., "Mechanical properties and microstructure of a graphene oxide–cement composite", ***Cement and Concrete Composites***, Vol. 58, (2015), 140-147. (https://doi.org/10.1016/j.cemconcomp.2015.02.001).
18. Wang, Y., Iqbal, Z. and Mitra, S., "Rapidly functionalized, water-dispersed carbon nanotubes at high concentration", ***Journal of the American Chemical Society***, Vol. 128 (2006), 95-99. (https://doi.org/10.1021/ja053003q).
19. Liu, C., Huang, X., Wu, Y., Deng, X., Liu, J., Zheng, Z. and Hui, D., "Review on the research progress of cement-based and geopolymer materials modified by graphene and graphene oxide", ***Nanotechnology Reviews***, Vol. 9, (2020), 155-169. (https://doi.org/10.1515/ntrev-2020-0014).
20. Anwar, A., Mohammed, B.S., Abdul Wahab, M. and Liew, M.S., "Enhanced properties of cementitious composite tailored with graphene oxide nanomaterial- A Review", ***Developments in the Built***

Environment, (2019), 1-43. (https://doi.org/10.1016/j.dibe.2019.100002).

21. Mohammed, A., Sanjayan, J.G., Duan, W. and Nazari, A., "Incorporating graphene oxide in cement composites: A study of transport properties", ***Construction and Building Materials***, Vol. 84, (2015), 341-347. (https://doi.org/10.1016/j.conbuildmat.2015.01.083).
22. Somasri, M. and Kumar, N.B., "Graphene oxide as nano material in high strength self-compacting concrete", ***Materials Today Proceedings***, Vol. 43, (2021), 2280-2289. (https://doi.org/10.1016/j.matpr.2020.12.1085).
23. Guo, K., Miao, H., Liu, L., Zhou, J. and Liu, M., "Effect of graphene oxide on chloride penetration resistance of recycled concrete", ***Nanotechnology Reviews***, Vol. 8, (2018), 681-689. (https://doi.org/10.1515/ntrev-2019-0059).
24. Birenboim, M., Nadiv, R., Alatawna, A., Buzaglo, M., Schahar, G. and Lee, J., "Reinforcement and workability aspects of graphene-oxide-reinforced cement nanocomposites", ***Composites Part B: Engineering***, Vol. 161, (2019), 68-76. (https://doi.org/10.1016/j.compositesb.2018.10.030).
25. Peng, H., Ge, Y., Cai, C., Zhang, Y. and Liu, Z., "Mechanical properties and microstructure of graphene oxide cement-based composites", ***Construction and Building Materials***, Vol. 194, (2019), 102-109. (https://doi.org/10.1016/j.conbuildmat.2018.10.234).
26. Xu, G., Du, S., He, J. and Shi, X., "The role of admixed graphene oxide in a cement hydration system", ***Carbon***, Vol. 148, (2019), 141-150. (https://doi.org/10.1016/j.carbon.2019.03.072).
27. Yang, H., Monasterio, M., Cui, H. and Han, N., "Experimental study of the effects of graphene oxide on microstructure and properties of cement paste composite" ***Composites Part A: Applied Science and Manufacturing***, Vol. 102, (2017), 263-272. (https://doi.org/10.1016/j.compositesa.2017.07.022).
28. Wang, Q., Wang, J., Lu, C.-X., Liu, B.-W., Zhang, K. and Li, C.-Z., "Influence of graphene oxide additions on the microstructure and mechanical strength of cement", ***New Carbon Materials***, Vol. 30, (2015), 349-356. (https://doi. org/10.1016/S1872-5805(15)60194-9).
29. Li, X., Lu, Z., Chuah, S., Li, W., Liu, Y., Duan, W.H. and Li, Z., "Effects of graphene oxide aggregates on hydration degree, sorptivity, and tensile splitting strength of cement paste", ***Composites Part A: Applied Science and Manufacturing***, Vol. 100 (2017), 1-8. (https://doi.org/10.1016/j. compositesa.2017.05.002).
30. Dikin, D.A., Stankovich, S., Zimney, E.J., Piner, R.D., Dommett, G.H.B., Evmenenko, G., Nguyen, S.T. and Ruoff, R.S., "Preparation and characterization of graphene oxide paper", ***Nature***, Vol. 448, (2007), 457-460. (https://doi.org/10.1038/ nature06016).
31. Li, X., Korayem, A.H., Li, C., Liu, Y., He, H., Sanjayan, J.G. and Duan, W.H., "Incorporation of graphene oxide and silica fume into cement paste: A study of dispersion and compressive strength", ***Construction and Building Materials***, Vol. 123, (2016), 327-335. (https://doi.org/10.1016/j.conbuildmat.2016.07.022).
32. Lu, L. and Ouyang, D., "Properties of cement mortar and ultra-high-strength concrete incorporating graphene oxide nanosheets", ***Nanomaterials***, Vol. 7, (2017), 187. (https://doi.org/10.3390/nano7070187).
33. Lv, S., Ma. Y., Qiu, C., Sun, T., Liu, J. and Zhou, Q., "Effect of graphene oxide nanosheets of microstructure and mechanical properties of cement composites", ***Construction and Building Materials***, Vol. 49, (2013), 121-127. (https://doi.org/10.1016/j.conbuildmat.2013.08.022).
34. Li, G.Y., Wang, P.M. and Zhao, X., "Mechanical behavior and microstructure of cement composites incorporating surface-treated multi-walled carbon nanotubes", ***Carbon***, Vol. 43, (2005), 1239-1245. (https://doi.org/10.1016/J.CARBON.2004.12.017).
35. Shang, Y., Zhang, D., Yang, C. and Liu, Y., "Effect of graphene oxide on the rheological properties of cement pastes", ***Construction and Building Materials***, Vol. 96, (2015) 20-28. (https://doi.org/10.1016/j.conbuildmat.2015.07.181).
36. Gong, K., Pan, Z., Korayem, A.H., Qiu, L., Li, D., Collins, F., Wang, C.M. and Duan, W.H., "Reinforcing effects of graphene oxide on portland cement paste", ***Journal of Materials in Civil Engineering***, Vol. 27, (2015), A4014010. (https://doi.org/10.1061/(ASCE)MT.1943-5533.0001125).
37. Lee, S., Jeong, H., Kim, D. and Won, J., "Graphene oxide as an additive to enhance the strength of cementitious composites", ***Composite Structures***, (2020), 1-27. (https://doi.org/10.1016/j.compstruct.2020.112154).
38. Kudžma, A., Škamat, J., Stonys, R., Krasnikovs, A., Kuznetsov, D., Girskas, G. and Antonovič, A., "Study on the effect of graphene oxide with low oxygen content on Portland cement based composites", ***Materials***, Vol. 12, (2019), 1-17. (https://doi:10.3390/ma12050802).
39. Hassani, A., Fakhim, B., Rashidi, A. and Ghoddousi, P., "The influence of graphene oxide on mechanical properties and durability increase of concrete pavement", ***International Journal of Transportation Engineering (IJTE)***, Vol. 2, (2014), 119-130. (http://www.ijte.ir/article_7874_1114.html).
40. Wang, L., Zhang, S., Zheng, D., Yang, H., Cui, H., Tang, W. and Li, D., "Effect of graphene oxide (GO) on the morphology and microstructure of cement hydration products", ***Nanomaterials***, Vol. 7, (2017), 1-10. (https://doi.org/10.3390/nano7120429).
41. Li, W., Li, X., Chen, S.J., Long, G., Liu, Y.M. and Duan, W.H., "Effects of nanoalumina and graphene oxide on early-age hydration and mechanical properties of cement paste", ***Journal of Materials in Civil Engineering***, Vol. 29, (2017), 1-9. (https://doi.org/10.1061/(ASCE))MT.1943-5533.0001926).
42. Silvestre, J., Silvestre, N. and De Brito, J., "Review on concrete nanotechnology", ***European Journal of Environmental and Civil Engineering***, Vol. 20, (2016), 455-485. (https://doi.org/10.1080/19648189.2015.1042070).
43. Bondar, D., Nanukuttan, S.V., Soutsos, M.N., Basheer, P.M. and Provis, J.L., "Suitability of alkali-activated GGBS/fly ash concrete for chloride environments", ***ACI Special Publications: American Concrete Institute***, Vol. 35, (2017), 1-14. (https://www.researchgate.net/publication/317950089_Suitability_of_alkali_activated_ggbsfly_ash_concrete_for_chloride_environments).
44. Du, H., Gao, H.J. and Dai S., "Improvement in concrete resistance against water and chloride ingress by adding graphene nanoplatelet", ***Cement and Concrete Research***, Vol. 83, (2016), 114-123. (https://doi.org/10.1016/j.cemconres.2016.02.005).
45. Xu, Y. and Fan, Y., "Effect of on graphene oxide the concrete resistance to chloride ion permeability", ***IOP Conference Series: Materials Science and Engineering: IOP Publishing,*** (2018), 032020. (https://doi.org/10.1088/1757-899X/394/3/032020).
46. Karri, S.K., Rao, G.R. and Raju, P.M., "Strength and durability studies on GGBS concrete", ***SSRG International Journal of Civil Engineering (SSRG-IJCE)***, Vol. 2, (2015), 34-41. (https://doi.org/10.14445/23488352/IJCE-V2I10P106).
47. Dalla, P.T., Tragazikis, I.K., Exarchos, D.A., Dassios, K.G., Barkoula, N.M. and Matikas. T.E., "Effect of carbon nanotubes on chloride penetration in cement mortars", ***Applied Sciences***, Vol. 9, (2019), 1032. (https://doi.org/10.3390/app9051032).
48. Song, H. and Saraswathy, V., "Studies on the corrosion resistance of reinforced steel in concrete with ground granulated blast-furnace slag-An overview", ***Journal of Hazardous Materials***, Vol. 138, (2006), 226-233. (https:// 10.1016/j.jhazmat.2006.07.022).
49. Richardson, D.N., "Strength and durability characteristics of a 70 % ground granulated blast furnace slag (GGBFS) concrete mix", (2006). (https://scholarsmine.mst.edu/cgi/viewcontent.cgi?article=1042&context=civarc_enveng_facwork).
50. Kumar, V.P., Gunasekaran, K. and Shyamala, T., "Characterization study on coconut shell concrete with partial replacement of cement by GGBS", ***Journal of Building Engineering***, (2019), 100830. (https://doi.org/10.1016/j.jobe.2019.100830).
51. Woo, H.M., Kim, C.-Y. and Yeon, J.H., "The heat of hydration and mechanical properties of mass concrete with high-volume GGBFS replacements", ***Journal of Thermal Analysis and Calorimetry***, Vol. 132, (2018), 599-609. (https://doi.org/10.1007/s10973-017-6914-z).
52. Özbay, E., Erdemir, M. and Durmuş, H.İ., "Utilization and efficiency of ground granulated blast furnace slag on concrete properties–A review", ***Construction and Building Materials***, Vol. 105, (2016), 423-434. (https://doi.org/10.1016/j.conbuildmat.2015.12.153).
53. Chen, H.-J., Huangm S.-S., Tang, C.-W., Malek, M.A. and Ean, L.-W., "Effect of curing environments on strength, porosity, and chloride ingress resistance of blast furnace slag cement concretes a construction site study", ***Construction and Building Materials***, Vol. 35, (2012), 1063-1070. (https://doi.org/10.1016/j.conbuildmat.2012.06.052).
54. Samad, S., Shah, A. and Limbachiya, M.C., "Strength development characteristics of concrete produced with blended cement using ground granulated blast furnace slag (GGBS) under various curing conditions", ***Sādhanā***, Vol. 42, (2017), 1203-1213. (https://doi.org/10.1007/s12046-017-0667-z).

55. Khatib, J. and Hibbert, J., "Selected engineering properties of concrete incorporating slag and metakaolin", ***Construction and Building Materials***, Vol. 19, (2005), 460-472. (https://doi.org/10.1016/j.conbuildmat.2004.07.017).
56. Shen, D., Jiao, Y., Kang, J., Feng, Z. and Shen, Y., "Influence of ground granulated blast furnace slag on the early-age cracking potential of internally cured high-performance concrete", ***Construction and Building Materials***, Vol. 233, (2020), 117083. (https://doi.org/10.1016/j.conbuildmat.2019.117083).
57. Güneyisi, E. and Gesoğlu, M., "A study on durability properties of high-performance concretes incorporating high replacement levels of slag", ***Materials and Structures***, Vol. 41, (2008), 479-493. (https://doi.org/10.1617/s11527-007-9260-y).
58. Park, J.-H. and Lee, H.-S., "Effect of curing condition on the chloride ion diffusion coefficient in concrete with GGBFS", ***Journal of the Korea Institute of Building Construction***, Vol. 19, (2019), 421-429. (https://doi.org/10.3390/ma12193233).
59. Yoon, Y.-S., Cho, S.-J. and Kwon, S.-J., "Prediction equation for chloride diffusion in concrete containing GGBFS based on 2-Year cured results", ***Journal of the Korea institute for structural maintenance and inspection***, Vol. 23, (2019), 1-9. (https://doi.org/10.11112/jksmi.2019.23.2.1).
60. Sharma, S. and Kothiyal, N.C., "Comparative effects of pristine and ball-milled graphene oxide on physico-chemical characteristics of cement mortar nanocomposites", ***Construction and Building Materials***, Vol. 115, (2016), 256-268. (https://doi.org/10.1016/j.conbuildmat.2016.04.019).
61. Mahendran, R., Sridharan, D., Santhakumar, K., Selvakumar, T., Rajasekar, P. and Jang, J.-H., "Graphene oxide reinforced polycarbonate nanocomposite films with antibacterial properties", ***Indian Journal of Materials Science***, (2016), 1-10. (https://doi.org/10.1155/2016/4169409).
62. Eigler, S. and Hirsch, A., "Chemistry with graphene and graphene oxide—challenges for synthetic chemists", ***Angewandte Chemie International Edition***, Vol. 53, (2014), 7720-7738. (https://doi.org/10.1002/anie.201402780).
63. Babak, F., Abolfazl, H., Alimorad, R. and Parviz, G., "Preparation and mechanical properties of graphene oxide: Cement nanocomposites", ***The Scientific World Journal***, (2014), 1-11. (https://doi.org/10.1155/2014/276323).
64. Guerrero-Contreras, J. and Caballero-Briones, F., "Graphene oxide powders with different oxidation degrees, prepared by synthesis variations of the Hummers method", ***Materials Chemistry and Physics***, Vol. 153, (2015), 209-220. (https://doi.org/10.1016/j.matchemphys.2015.01.005).
65. Male, U., Srinivasan, P. and Singu, B.S., "Incorporation of polyaniline nanofibres on graphene oxide by interfacial polymerization pathway for supercapacitor", ***International Nano Letters***, Vol. 5, (2015), 231-240. (https://doi.org/10.1007/s40089-015-0160-90).
66. Hemidouche, S., Boudriche, L., Boudjemaa, A. and Hamoudi, S., "Removal of lead (II) and cadmium (II) cations from water using surface-modified graphene", ***The Canadian Journal of Chemical Engineering***, Vol. 95, (2017), 508-515. (https://doi.org/10.1002/cjce.22693).
67. ASTM C1202, Standard test method for electrical indication of concrete's ability to resist chloride ion penetration, Annual Book of ASTM Standards, (2012). (https://www.astm.org/Standards/C1202).
68. Lataste, J., Sirieix, C., Breysse, D. and Frappa, M., "Electrical resistivity measurement applied to cracking assessment on reinforced concrete structures in civil engineering", ***NDT & E International***, Vol. 36, (2003), 383-394. (https://doi.org/10.1016/S0963-8695(03)00013-6).
69. Azarsa, P. and Gupta, R., "Electrical resistivity of concrete for durability evaluation: A review", ***Advances in Materials Science and Engineering***, (2017), 1-9. (https://doi.org/10.1155/2017/8453095).
70. Yang, H.-M., Kwon, S.-J., Myung, N.V., Singh, J.K., Lee, H.-S. and Mandal, S., "Evaluation of strength development in concrete with ground granulated blast furnace slag using apparent activation energy", ***Materials***, Vol. 13, (2020), 442. (https://doi.org/10.3390/ma13020442).
71. Oner, A. and Akyuz, S., "An experimental study on optimum usage of GGBS for the compressive strength of concrete", ***Cement and Concrete Composites***, Vol. 29, (2007), 505-514. (https://doi.org/10.1016/j.cemconcomp.2007.01.001).
72. Zhao, H., Sun, W., Wu, X. and Gao, B., "The properties of the self-compacting concrete with fly ash and ground granulated blast furnace slag mineral admixtures", ***Journal of Cleaner Production***, Vol. 95, (2015), 66-74. (https://doi.org/10.1016/j.jclepro.2015.02.050).
73. Muhmood, L., Vitta, S. and Venkateswaran, D., "Cementitious and pozzolanic behavior of electric arc furnace steel slags", ***Cement and Concrete Research***, Vol. 39, (2009), 102-109. (https://doi.org/10.1016/j.cemconres.2008.11.002).
74. Li, X., Liu, Y.M., Li, W.G., Li, C.Y., Sanjayan, J.G. and Duan, W.H., "Effects of graphene oxide agglomerates on workability, hydration, microstructure, and compressive strength of cement paste", ***Construction and Building Materials***, Vol. 145, (2017), 402-410. (https://doi.org/10.1016/j.conbuildmat.2017.04.058).
75. Li, M. and Kim, J.-M., "Strength properties and microstructure of steel slag-based hardened cementitious composite with graphene oxide", ***MATEC Web of Conferences: EDP Sciences***, (2017), 03012. (https://doi.org/10.1051/matecconf/201713803012).
76. Yu, L., Jiang, L., Chu, H., Guo, M., Zhu, Z. and Dong, H., "Effect of electrochemical chloride removal and ground granulated blast furnace slag on the chloride binding of cement paste subjected to NaCl and Na_2SO_4 attack", ***Construction and Building Materials***, Vol. 220, (2019), 538-546. (https://doi.org/10.1016/j.conbuildmat.2019.06.033).
77. Dhir, R., El-Mohr, M. and Dyer, T., "Chloride binding in GGBS concrete", ***Cement and Concrete Research***, Vol. 26, (1996), 1767-1773. (https://doi.org/10.1016/S0008-8846(96)00180-9).
78. Luo, R., Cai, Y., Wang, C. and Huang, X., "Study of chloride binding and diffusion in GGBS concrete", ***Cement and Concrete Research***, Vol. 33, (2003), 1-7. (https://doi.org/10.1016/S0008-8846(02)00712-3).
79. Khan, M. and Kayali, O., "Chloride binding ability and the onset corrosion threat on alkali-activated GGBFS and binary blend pastes", ***European Journal of Environmental and Civil Engineering***, Vol. 22, (2018), 1023-1039. (https://doi.org/10.1080/19648189.2016.1230522).
80. Chi, M.C., Chi, J.H. and Wu, C.H., "Effect of GGBFS on compressive strength and durability of concrete", ***Advanced Materials Research: Trans. Tech. Publ.***, Vol. 1145, (2018), 22-26. (https://doi.org/10.4028/www.scientific.net/AMR.1145.22).
81. Jang, S., Karthick, S. and Kwon, S., "Investigation on durability performance in early aged high-performance concrete containing GGBFS and FA", ***Advances in Materials Science and Engineering***, (2017), 1-11. (https://doi.org/10.1155/2017/3214696).
82. Cheng, A., "Influence of GGBS on durability and corrosion behavior of reinforced concrete", ***Materials Chemistry and Physics***, Vol. 93, (2005), 404-411. (https://doi.org/10.1016/j.matchemphys.2005.03.043).
83. Guo, K., Miao, H., Liu, L., Zhou, J. and Liu, M., "Effect of graphene oxide on chloride penetration resistance of recycled concrete", ***Nanotechnology Reviews***, Vol. 8, (2019), 681-689. (https://doi.org/10.1515/ntrev-2019-0059).